

HIERARCHICAL GALAXY FORMATION AND SUBSTRUCTURE IN THE GALAXY'S STELLAR HALO

JAMES S. BULLOCK¹, ANDREY V. KRAVTSOV² AND DAVID H. WEINBERG

Department of Astronomy, The Ohio State University, 140 W. 18th Ave, Columbus, OH 43210-1173

Astrophysical Journal, submitted

ABSTRACT

We develop an explicit model for the formation of the stellar halo from tidally disrupted, accreted dwarf satellites in the cold dark matter (CDM) framework, focusing on predictions testable with the Sloan Digital Sky Survey (SDSS) and other wide-field surveys. Subhalo accretion and orbital evolution are calculated using a semi-analytic approach based on the extended Press-Schechter formalism. Motivated by our previous work, we assume that low-mass subhalos ($v_c < 30 \text{ km s}^{-1}$) can form significant populations of stars only if they accreted a substantial fraction of their mass before the epoch of reionization. With this assumption, the model reproduces the observed velocity function of galactic satellites in the Local Group, solving the “dwarf satellite problem” without modifying the basic tenets of the popular Λ +CDM cosmological scenario. The tidally disrupted satellites in this model yield a stellar distribution whose total mass and radial density profile are consistent with those observed for the Milky Way stellar halo. Most significantly, the model predicts the presence of many large-scale, coherent substructures in the outer halo. These substructures are remnants of individual, tidally disrupted dwarf satellite galaxies. Substructure is more pronounced at large galactocentric radii because of the smaller number density of tidal streams and the longer orbital times. This model provides a natural explanation for the coherent structures in the outer stellar halo found in the SDSS commissioning data, and it predicts that many more such structures should be found as the survey covers more of the sky. The detection (or non-detection) and characterization of such structures could eventually test variants of the CDM scenario, especially those that aim to solve the dwarf satellite problem by enhancing satellite disruption.

Subject headings: cosmology: theory – galaxies:formation

1. INTRODUCTION

The origin of the Milky Way’s stellar halo is a long-standing astronomical problem. The poles of the debate are defined by the monolithic collapse model of Eggen, Lynden-Bell, & Sandage (1962) and the chaotic accretion model of Searle (1977) and Searle & Zinn (1978). The Searle & Zinn picture has gained currency in recent years in part because of growing recognition that the halo and bulge are distinct components that may have different formation mechanisms (see, e.g., the reviews by Wyse 1999ab) and in part because of “smoking gun” evidence that includes the tidally distorted Sagittarius dwarf galaxy (Ibata et al. 2000a and references therein) and the presence of extra-tidal stars around many dwarf spheroidal satellites (Gould et al. 1992; Irwin & Hatzidimitriou 1995; Kuhn, Smith & Hawley 1996). The Searle & Zinn scenario also bears a strong anecdotal resemblance to the hierarchical galaxy formation scenario characteristic of inflationary cold dark matter (CDM) cosmological models. In this paper, we make the connection between CDM cosmology and hierarchical stellar halo formation much more explicit, by presenting a simple but quantitative model for halo formation in the CDM framework and obtaining predictions for the degree of residual substructure in the outer halo.

Previous studies of stellar halo formation in the hierarchical framework have focused on the fossil evidence for satellite disruption preserved in phase space substructure

of the halo stars (e.g., Johnston, Spergel & Hernquist 1995; Helmi & White 1999). These studies were aimed primarily at exploiting surveys of the halo in the solar neighborhood (e.g., Arnold & Gilmore 1992; Preston, Beers & Shectman 1994; Majewski, Munn & Hawley 1994, 1996). Wide-angle, deep, multi-color surveys, such as the Sloan Digital Sky Survey (SDSS; York et al. 2000), open up new avenues for studying the structure of the stellar halo. RR Lyrae stars, detected by their variability and color, can provide a three-dimensional map of the distribution of halo stars. The more general population of A-colored halo stars can be used for the same purpose; relative to RR Lyrae they have the advantages of greater numbers and detectability in a single observation epoch but the disadvantage of being less precise standard candles. Studies of RR Lyrae stars and A-colored stars in SDSS commissioning data have already revealed two large substructures in the outer halo (Ivezić et al. 2000; Yanny et al. 2000). The photometric depth of the SDSS and the intrinsic brightness of RR Lyrae and A stars allows a probe of halo structure out to large distances, $\sim 75 \text{ kpc}$, and the restricted absolute-magnitude range of RR Lyrae and A stars prevents 3-dimensional substructure from being washed out by projection. Carbon star surveys (e.g., Ibata et al. 2000a) and surveys of giant stars (Majewski et al. 2000) offer similar prospects.

The model presented in this paper is an extension of our previous work aimed at explaining the observed abun-

¹james,andrey,dhw@astronomy.ohio-state.edu

²Hubble Fellow

dance of dwarf satellite galaxies in the Local Group within the CDM framework (Bullock, Kravtsov & Weinberg 2000; hereafter BKW). In BKW we showed that the observed shape and amplitude of the velocity function of dwarf satellite galaxies in the Local Group can be explained if gas accretion and star formation are suppressed in low-mass dark matter clumps after intergalactic gas is reheated during the epoch of reionization. In this picture, the observed dwarf satellites around our Galaxy are those that assembled a large fraction of their mass before reionization *and* survived the decay of their orbit as a result of dynamical friction *and* avoided tidal disruption by the Milky Way potential. As shown in Fig. 1 of BKW, the number of tidally disrupted objects is similar to the number of surviving dwarf satellites. Here we show that the disrupted satellites produce a population of stars whose total mass and radial profile are consistent with observations of the Milky Way’s stellar halo. In the outer halo, where the number of contributing satellites is relatively small and the orbital times are long, the model predicts substantial substructure, which should be detectable with the SDSS and other deep, wide-angle surveys.

Our model is simple and is unlikely to be accurate in full quantitative detail. However, the qualitative predictions should be characteristic of conventional CDM cosmologies combined with straightforward assumptions about the star formation in low-mass dark matter potential wells. If the observed stellar halo is found to be radically different from these predictions, it will mean that either our star formation assumptions or the CDM predictions for hierarchical small-scale structure in the dark matter distribution are incorrect. In this sense, studies of the stellar distribution in the outer halo can play a valuable role in testing more general ideas about galaxy formation.

For convenience, we will focus on predictions for the RR Lyrae distribution. RR Lyrae are especially useful probes of the stellar halo because they are relatively easy to identify, they are luminous enough to be detected out to large distances ($r \sim 100$ kpc), and they are nearly standard candles and therefore yield 3-dimensional maps. RR Lyrae are believed to be good tracers of the more general halo stellar distribution, and they have often been used in kinematic studies of the halo (Hawkins 1984). Finally, while RR Lyrae are numerous enough to trace halo substructure, they are rare enough that we can construct numerical realizations that contain every individual RR Lyrae star. The stellar density fluctuations predicted by our model are far in excess of Poisson fluctuations, so it is straightforward to scale our predictions to other halo tracers like blue horizontal branch stars or carbon stars, just by putting in appropriate stellar population weights.

The remainder of the paper is organized as follows. In § 2 we will describe our model and assumptions. Specifically, we will describe our semi-analytic method for following the accretion and orbital evolution of satellite galaxies in § 2.1 and our modeling of stellar debris of disrupted satellites in § 2.2. We present our results in § 3. We finish with discussion and conclusions in § 4.

2. METHOD

2.1. Accretion and orbital evolution of satellites

We use a semi-analytic method to trace the accretion history and orbital evolution of satellite galaxies within a typical Milky Way-size dark halo.³ Detailed description of the model is given in BKW. Here, we briefly review its essential aspects. The model uses the extended Press-Schechter formalism (Bond et al. 1991; Lacey & Cole 1993) to construct the accretion history for each galactic halo. The mass of a halo in this formalism is accumulated via accretion of individual *subhalos* of different masses, and we keep track of all the accreted subhalos down to some minimum mass. The second part of our model is a semi-analytic prescription for orbital evolution of the accreted subhalos. This prescription is used to determine whether a subhalo survives to the present day, is tidally disrupted, or is dragged into the central galaxy by dynamical friction. Only subhalos that accreted a significant fraction ($\geq 0.2 - 0.3$) of their mass before intergalactic gas was reheated during the epoch of reionization are assumed to host luminous galaxies. In the model presented in this paper, the stellar halo of Milky Way-like galaxies is formed from the debris of those subhalos that once hosted luminous galaxies but were tidally disrupted before the present day. For our analysis, we adopt a flat CDM model with a non-zero vacuum energy and the following parameters: $\Omega_m = 0.3$, $\Omega_\Lambda = 0.7$, $h = 0.7$, $\sigma_8 = 1.0$, where σ_8 is the rms fluctuation on the scale of $8h^{-1}$ Mpc, h is the Hubble constant in units of $100 \text{ km s}^{-1} \text{ Mpc}^{-1}$, and Ω_m and Ω_Λ are the density contributions of matter and the vacuum respectively in units of the critical density.

We assume that the density profile of each dark matter halo is described by the NFW profile (Navarro, Frenk, & White 1997): $\rho_{\text{NFW}}(x) \propto x^{-1}(1+x)^{-2}$, where $x = r/r_s$, and r_s is a characteristic inner radius. Given a halo of mass M_{vir} at redshift z , the model of Bullock et al. (2000a) supplies the typical r_s value and specifies the profile completely. The circular velocity curve, $v^2(r) \equiv GM(r)/r$, peaks at a value v_m at a radius $r_m \simeq 2.16r_s$.

We use the merger tree method of Somerville & Kolatt (1999) to construct mass growth and halo accretion histories for an ensemble of galaxy-sized dark matter halos. We start with halos of mass $M_{\text{vir}} = 1.1 \times 10^{12} h^{-1} M_\odot$, at $z = 0$, and trace subhalo accretion histories back to $z = 10$. We record the mass growth for the primary halo, $M_{\text{vir}}(z)$, as well as the mass of each accreted subhalo, M_a , and the time of its accretion, t_a (or z_a). We assign the subhalo v_m according to the mass-velocity relation at the epoch of accretion. For the results presented below, we use 100 ensembles of formation histories for galactic host halos. We obtain very similar results if this number is increased.

Each subhalo is assigned an initial orbital circularity, ϵ , defined as the ratio of the angular momentum of the subhalo to that of a circular orbit with the same energy, $\epsilon \equiv J/J_c$. We choose ϵ randomly in the range $0.1 - 1.0$ (Ghigna et al. 1998). To determine whether the accreted halo’s orbit will decay, we use Chandrasekhar’s formula to calculate the decay time, τ_{DF}^D , of the orbit’s circular radius

³In this paper, the term “halo” sometimes refers to a dark matter halo and sometimes to a stellar halo. Usually the meaning is clear from context, but we will specify “dark” or “stellar” where necessary. The term “subhalo” always refers to a dark matter halo, one that is accreted into a larger dark matter halo before redshift zero.

r_c — the radius of a circular orbit with the same energy as the actual orbit. Each subhalo is assumed to start at a randomly assigned radius $r_c^a = (0.4 - 0.75)R_{\text{vir}}(t_a)$, where $R_{\text{vir}}(t_a)$ is the virial radius of the host halo at the time of accretion. We determined this distribution of circular radii by measuring the range of binding energies of subhalos in the ART simulations used by Klypin et al (1999a). Once τ_{DF}^c is known, the decay time for the given circularity is $\tau_{DF} = \tau_{DF}^c \epsilon^{0.4}$ (Colpi et al. 1999). If τ_{DF} is smaller than the time left between accretion and $z = 0$, $\tau_{DF} \leq t_0 - t_a$, then the subhalo will merge with the central object. In our modeling of the stellar halo, we do not consider the contribution due to galaxies that subsequently merge with the central object. Due to the rapid decay of the orbits, any debris associated with these objects will likely remain confined within the radius where stripping first becomes important, typically $r \lesssim 10$ kpc. For this reason, we consider the predictions for the stellar distribution only for galactocentric radii $r > 10$ kpc.

If τ_{DF} is too long for the orbit to have decayed completely ($\tau_{DF} > t_0 - t_a$), we check whether the subhalo would have been tidally disrupted. We assume that the halo is disrupted if the tidal radius becomes smaller than r_m . The tidal radius, r_t , is determined at the pericenter of the orbit at $z = 0$, where the tides are the strongest, following Klypin et al. (1999b). If $r_t \leq r_{\text{max}}$ we declare the subhalo to be tidally destroyed and record its mass and orbital parameters so that we may model the evolution of its tidal debris (§2.2).

The resulting average mass functions for all accreted halos and the subset of the halos that were tidally disrupted are shown in Figure 1 with the thin dashed and solid lines, respectively. The error bars represent the run-to-run dispersion over 100 realizations. For comparison, the dotted line corresponds to halos that were dragged to the halo center as a result of dynamical friction. As expected, the dynamical friction is more efficient for massive subhalos. The mass function of surviving subhalos is similar to that of the disrupted halos, but we omit it here to preserve visual clarity.

As in BKW, we assume that of all subhalos with $v_m < 30 \text{ km s}^{-1}$ only those that accreted a fraction f of their gas before the redshift of reionization, z_{re} , host luminous galaxies. Although our results are consistent with the observed abundance of dwarf satellites for a range of values of f and z_{re} , here we use the fiducial values of BKW, $f = 0.3$ and $z_{\text{re}} = 8$. We expect that our results for disrupted satellites would be similar if we chose other f , z_{re} combinations that also match the observed (surviving) dwarf satellite population. For a given subhalo of mass M_a and accretion redshift z_a , we use equation (2.26) of LC93 to probabilistically assign the redshift, z_f , at which the main progenitor of the subhalo reached mass $M_f = fM_a$ for the first time. The subhalo hosts a luminous galaxy only if $z_f \geq z_{\text{re}}$. We also assume that subhalos with $v_m < v_l = 10 \text{ km s}^{-1}$ do not host galaxies, since any gas that was initially accreted in these small systems would be unable to cool, and it should quickly boil out of the halo after reionization (e.g., Barkana & Loeb 1999). Our results do not change if we vary v_l by 50%. The thick solid line in Figure 1 shows the average mass function of disrupted halos that once hosted luminous galaxies. The mass function of the surviving galaxies is similar to that of the disrupted galaxies, but

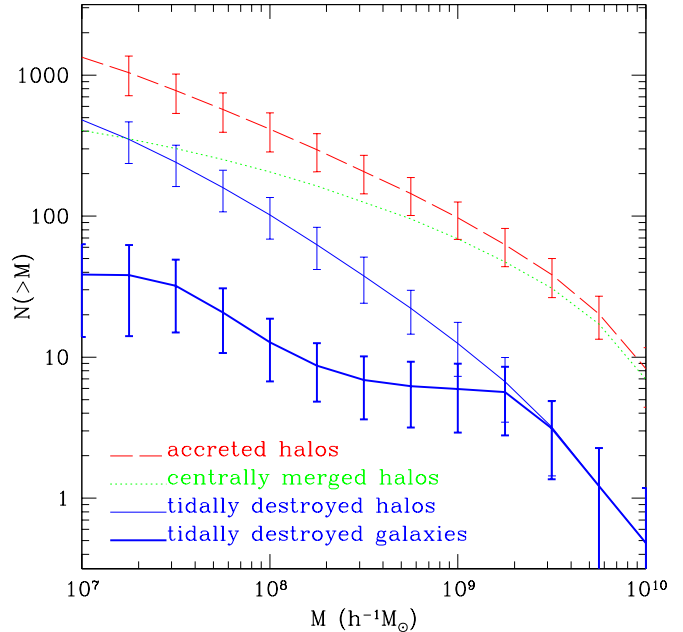


FIG. 1.— Cumulative mass function of all accreted dark matter subhalos (*dashed line*), the fraction that decayed due to dynamical friction (*dotted line*), tidally disrupted halos (*thin solid line*), and the fraction of disrupted halos that host galaxies (*thick solid line*). Not shown is the mass function of surviving halos, which is similar to that of disrupted halos, and the mass function of surviving *galaxies*, which is roughly half that of the disrupted galaxies (reflecting the tendency for surviving halos to have been accreted later). The mass function represents the average over 100 merger histories for host halos of mass $M_{\text{vir}}(z = 0) = 1.1 \times 10^{12} h^{-1} M_{\odot}$. The errorbars show the dispersion over the different merger histories.

lower in amplitude by about a factor of two. Surviving halos are typically accreted later than tidally destroyed halos, and they are less likely to form before reionization and host a galaxy.

2.2. Modeling stellar tidal debris

Estimating the number of tidally stripped stars, and RR Lyrae stars in particular, requires several uncertain assumptions about gas cooling, star formation, and stellar population morphology. The following approximations are extremely simplified, and the estimated number of disrupted stars for each object is uncertain at the factor of 2–3 level. This uncertainty is passed on to the overall amplitude of calculated stellar density distribution in the halo. Nevertheless, our statistical measures of substructure depend only on the ratio to the background density, and they are thus largely insensitive to the precise values we assume. Furthermore, we adopt the same assumptions that we used in BKW to obtain consistency with the observed dwarf satellite population, and this matching normalizes out some of the uncertainties in the overall stellar halo amplitude.

We estimate the luminosity of every disrupted luminous galaxy assuming that it has a baryonic mass $fM_a(\Omega_b/\Omega_m)$ (the mass of baryons accreted at $z > z_{\text{re}}$). We assume that a fraction ϵ_* of this baryonic mass is converted to a stel-

lar population with mass-to-light ratio M_*/L_V . The total mass to light ratio of the subhalo is thus

$$\left(\frac{M_{\text{vir}}}{L_V}\right) = f^{-1} \left(\frac{\Omega_m}{\Omega_b}\right) \left(\frac{M_*}{L_V}\right) \epsilon_*^{-1}. \quad (1)$$

Adopting $M_*/L_V \simeq 0.7$, typical for galactic disk stars (e.g., Binney & Merrifield 1998), $\Omega_m/\Omega_b \simeq 7$ (based on $\Omega_m = 0.3$, $h = 0.7$, and $\Omega_b h^2 \simeq 0.02$ from Burles & Tytler 1998), and $\epsilon_* = 0.5$, we obtain $(M/L_V) \simeq 10f^{-1} \simeq 33$. We estimate the number of horizontal branch stars in each galaxy using $N_{HB} = L_V/(540L_\odot)$ (Preston, Shectman, & Beers 1991). The fraction of the horizontal branch stars that are RR Lyrae variables is strongly dependent on the metallicities and ages of the populations, and it will vary significantly from one object to another. For simplicity, we assume that all disrupted objects have $N_{RR} = 0.3N_{HB}$. This fraction is high compared to local halo stars, but it is consistent with fractions observed for more distant ($r \gtrsim 10$ kpc) globular clusters, likely reflecting the tendency for the outer halo to be younger (Preston et al. 1991; Brocato et al. 1996; Layden 1998).

For each disrupted luminous subhalo, we randomly assign a direction for its angular momentum vector. This direction fixes the plane of the orbit since we assume that the dark halo potential is spherical (i.e., no orbital precession). We follow the orbit from the time it was accreted at t_a to t_0 using

$$\frac{dr}{dt} = \pm v(r_c) \sqrt{\frac{2}{v^2(r_c)} [\Phi(r_e) - \Phi(r)] + 1 - \frac{\epsilon^2 r_c^2}{r^2}}, \quad (2)$$

$$\frac{d\psi}{dt} = \frac{v(r_c) r_c \epsilon}{r^2}, \quad (3)$$

where r is the distance to the galactic center, ψ is the angle in the orbital plane, $\Phi(r) = -4.6v_m^2 \ln(1+x)/x$ is the potential of the host, and the \pm sign signifies whether the object is approaching its apocenter or pericenter, respectively. We will work in the approximation that the dynamical friction timescale is long compared to the time remaining for the orbital evolution and disruption: $\tau_{DF} \gg t_0 - t_a$. This is a good approximation for $\sim 90\%$ of the disrupted halos — not surprisingly, since we have deliberately restricted our analysis to halos whose orbits have not decayed (i.e., long τ_{DF}). In order to approximately account for cases where this approximation breaks down, we start integrating the satellite orbit at $t = t_a$ but set its starting radius equal to the circular radius it will have decayed to by $t = t_0$: $r(t_a) = r_c(t_0) \equiv r_c$. The initial value for the angle, $\psi(t_a)$, is chosen randomly, and we assume that the satellite is initially infalling (approaching the pericenter).

We assume that the satellite is tidally disrupted after the first passage of its orbit pericenter. At this time, the tidal debris will obtain an energy distribution from the encounter. Our model for the evolution of the debris along the tidal tail is motivated by numerical results of Johnston (1998), who showed that the following approximations provide good description of the positions of stripped particles in her simulations. The typical energy scale of the debris is set by the change in the host halo potential energy over the size of the tidally disrupted object,

$$\epsilon = r_t \frac{d\Phi}{dr} \simeq v_m^2 \left(\frac{r_t}{r_p}\right), \quad (4)$$

where r_p is the pericenter radius of the orbit. The last approximation is exactly true for a logarithmic potential (a singular isothermal density profile). We assume that the satellite is completely disrupted after the first passage, and that the energy of the debris is evenly distributed over the energy range $-\epsilon > dE > \epsilon$ (Evans & Kochanek 1989). This assumption ignores the possibility of disruption over several orbits, but we find that our results are robust to the choice of distribution and do not change significantly if the energy range is altered by 50%. Using intuition gained from a circular orbit within a singular isothermal density background, we may estimate how a change in energy from E to $E + dE$ affects the orbit of a particle. In this approximation, the azimuthal period, T_ψ , and radial period, T_r , depend only on the orbit energy, and they are both increased or decreased depending on the sign of the deposited energy: $T_{\psi,r}(E + dE) = \tau T_{\psi,r}(E)$, where

$$\tau = \exp\left(\frac{dE}{v_m^2}\right). \quad (5)$$

This result allows us to map the orbital trajectory of the initial object with energy E (Eqs. 4 and 5) to that of a debris particle with energy $E + dE$ via $[r(t), \psi(t)] \rightarrow [r(t/\tau), \psi(t/\tau)]$.

For each RR Lyrae star in the disrupted galaxy, we assign a change in energy dE and integrate the orbital equations to determine its position at $z = 0$. Since the disrupted galaxy will have some finite spherical extent, we add a random offset to this calculated central orbit position. The magnitude of this offset is a Gaussian deviate with dispersion 2 kpc, the typical optical radius for a dwarf galaxy (Mateo 1998), and the direction is random.

3. RESULTS

Figures 2 and 3 show two realizations of the RR Lyrae distribution from disrupted satellites in sky-projected galactic coordinates. The panels in each figure correspond to the indicated radial bins in galacto-centric radius. Qualitatively, it is clear that substructures become more pronounced at larger radii. This radial trend reflects the smaller number of disrupted satellites with large apocenters and the longer periods of their orbits, which reduces the extent of debris spreading along the orbit. A comparison of the maps in Figures 2 and 3 illustrates the differences between different merger histories of the host halo. One can see that the stochastic variations in merger history at fixed host mass lead to substantial variations in the appearance and abundance of substructures.

In light of the SDSS results referred to in § 1, the most interesting predictions of the model are the radial number density profile of halo stars and the clumpiness and spatial extent of the stellar distribution. Figure 4 shows radial number density profiles of the halo RR Lyrae stars. The long dashed lines in each panel represent the power law ($n_* \propto r^{-3}$) RR Lyrae density profile derived by Wetterer & McGraw (1996), based on their large compilation of RR Lyrae. The solid points show the profile computed

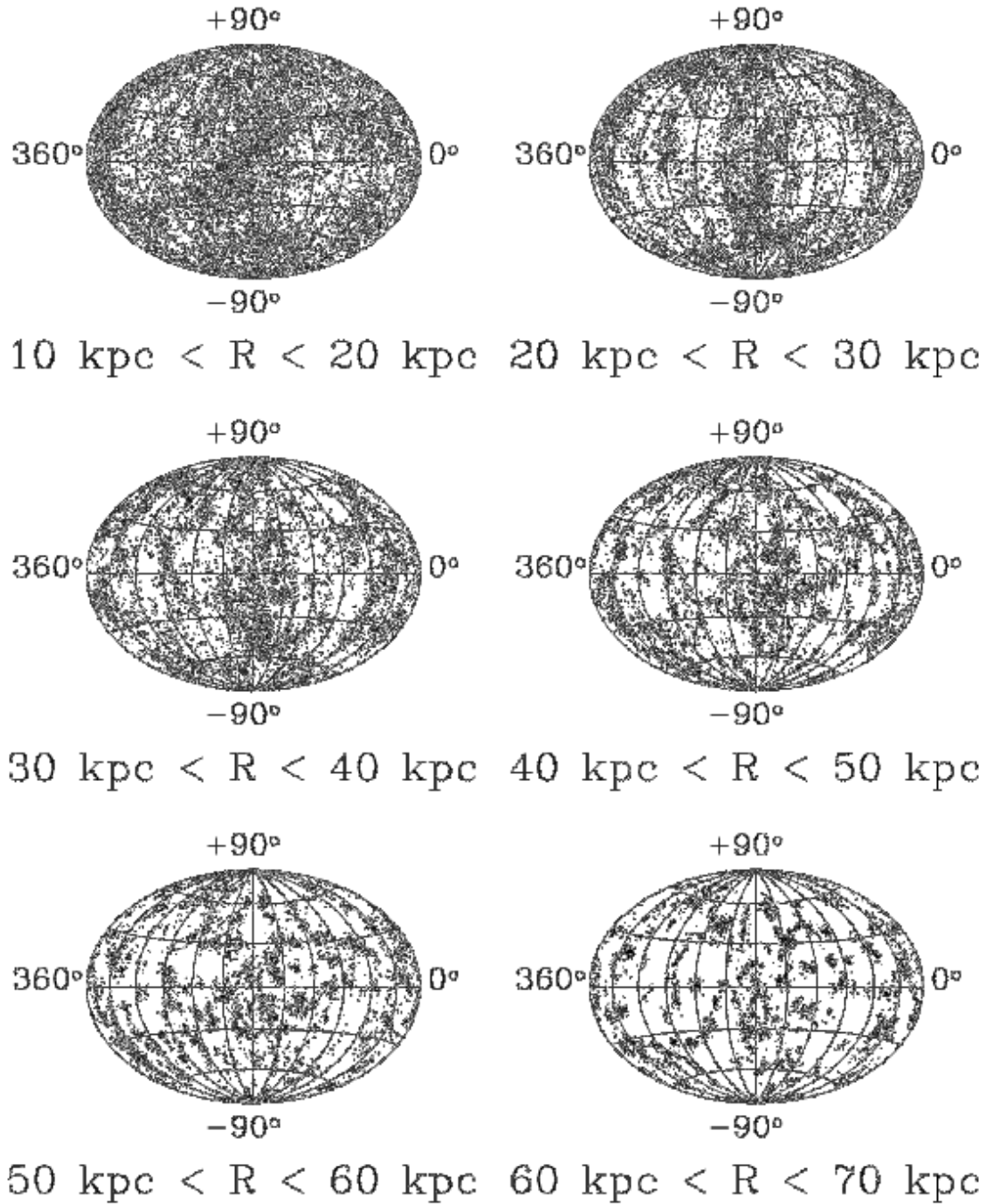


FIG. 2.— Distribution of stripped stars in various radial bins projected on the sky. Each point represents an RR Lyrae star, and the number of stars in each radial bin, starting in the upper left panel, is 11331, 9052, 8237, 7182, 6173, and 5076. These views are centered on the Galactic Center, but shifting to a solar origin makes no qualitative difference.

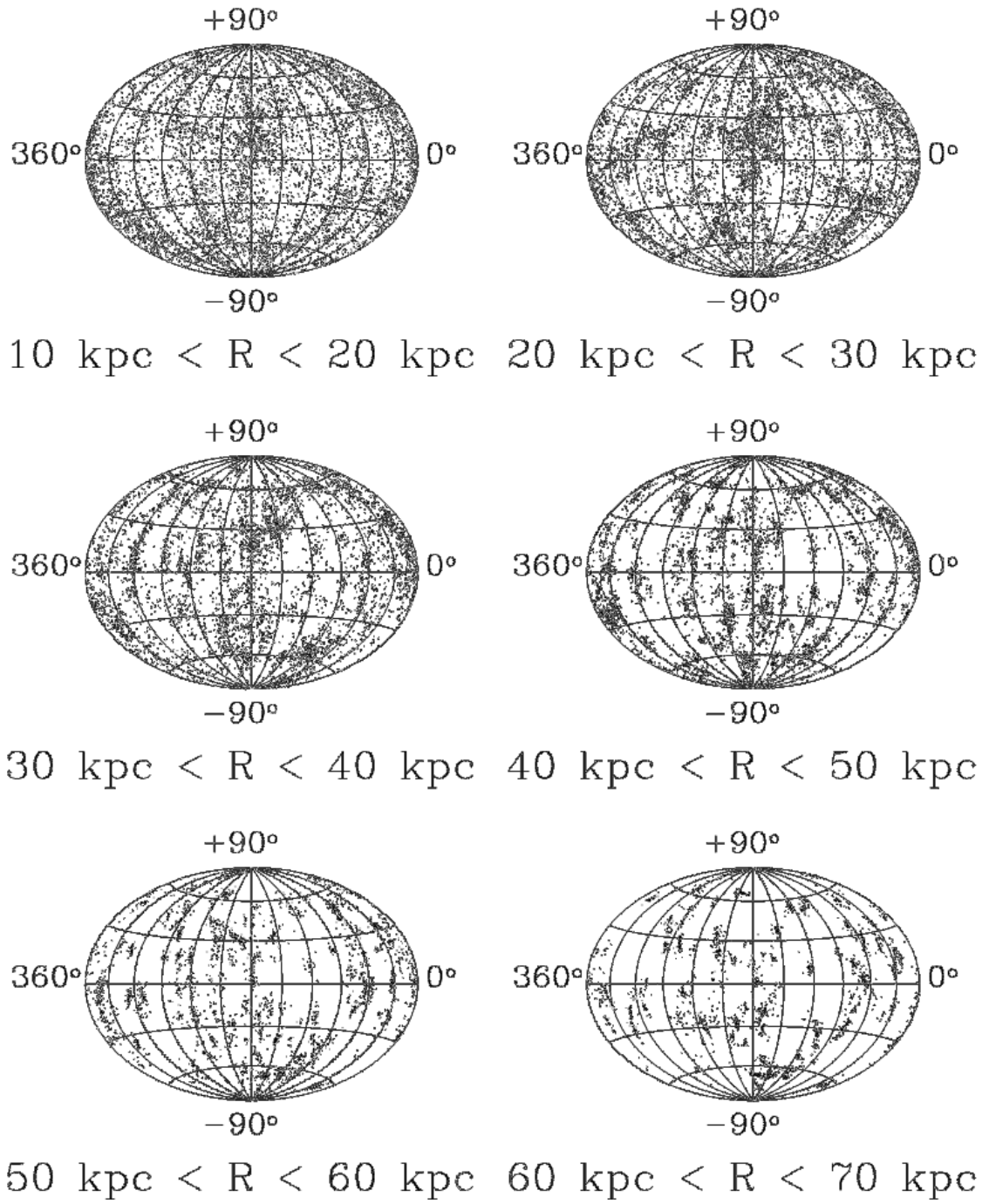


FIG. 3.— Same as Figure 2, but for a different merger history realization. Each point represents an RR Lyrae, and the number of stars in each radial bin, starting in the the upper left panel, is 6511, 6402, 4962, 4363, 2783, and 2077.

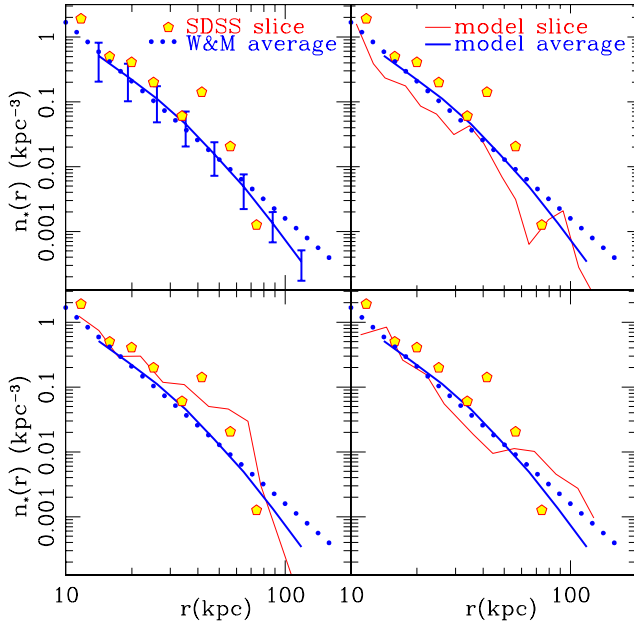


FIG. 4.— The average RR Lyrae density profile (thick solid line) compared with the Ivezić et al. (2000) SDSS data (solid points) and the power law determined by Wetterer & McGraw (1996) (dashed line). In the upper left panel, the error bars reflect the dispersion in the average from realization to realization. The thin solid lines in the other three panels are results of random strips similar in solid angle and geometry to the strips used to obtain the SDSS measurements (~ 1 degree wide, 100 square degree strip).

by Ivezić et al. (2000) for their sample of RR Lyrae candidates obtained from SDSS commissioning data, which covers roughly a one-degree wide, 100 square degree strip of sky. Note that the SDSS and Wetterer & McGraw profiles agree well at $\lesssim 35$ kpc. At larger radii, however, the SDSS sample shows two significant deviations from the smooth $n_* \propto r^{-3}$ profile: a “bump” in number density at $r \approx 40$ kpc and a sharp drop at $r \gtrsim 50$ kpc. As noted by Ivezić et al., this structure in the radial profile likely indicates significant clumpiness of the stellar halo at these galactocentric radii, and the bump in particular is associated with an identifiable coherent structure containing ~ 70 RR Lyrae within the observed region.

The model predictions are shown in Figure 4 by thick and thin solid lines. The thick solid lines represent the computed RR Lyrae number density profile averaged over all merging history realizations and the full sky. The error bars in the upper left panel show the dispersion from realization to realization around this average, demonstrating that stochastic variations in merger histories lead to a factor of ~ 2 rms variation in the overall normalization of the predicted halo density profile. In the remaining three panels, the thin solid lines show examples of density profiles derived from a single host halo realization, viewed through three randomly chosen strips similar in solid angle and geometry to the strips used to derive the SDSS sample.

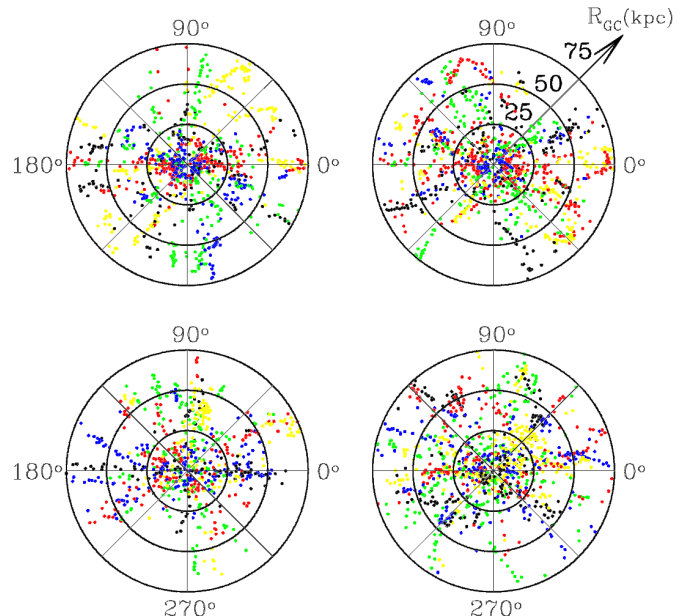


FIG. 5.— The radial distributions of disrupted RR Lyrae stars in 1 degree wide, great circle slices through a single model halo realization. This halo formed from about 60 disrupted satellites. Shown are four random cuts of great circle planes through the halo center. Each point represents a single RR Lyrae star. Concentric circles indicate galactocentric radii of 25, 50, and 75 kpc. Note that apparent “clumpiness” of the stellar distribution increases with increasing radius.

The first remarkable feature of Figure 4 is the agreement of the predicted average profile with the slope and amplitude found by Wetterer & McGraw (1996). As discussed in §2.2, the predicted amplitude is uncertain by a factor of several, and even the statistical fluctuations from one galaxy to another are significant, so the degree of agreement must be somewhat fortuitous. However, it is worth noting that we did not adjust any parameters to fit the observed halo profile but chose “best guess” values based on other considerations — in particular, the requirement of matching the observed dwarf satellite population. Figure 4 suggests that disruption of accreted satellites can produce not just substructure in the stellar halo but the entire stellar halo itself. If we have overestimated the number of RR Lyrae per unit dark matter mass, then there is room for another physical mechanism that creates a smooth underlying halo, but it seems that no such additional mechanism is necessary.

The second remarkable feature of Figure 4 is the jaggedness of the observed and predicted profiles of individual strips, which becomes especially pronounced at radii $r \gtrsim 40$ kpc. These large fluctuations reflect the substructure visible in Figures 2 and 3. The step drop in the SDSS counts between 60 and 70 kpc suggests detection of an “edge” of the stellar halo (Ivezić et al. 2000). However, the second of our numerical realizations shows an equally sharp edge, even though the average halo profile is smooth. Our model predicts a gradual steepening of the halo profile at $r \gtrsim 60$ kpc, but although surveys in small solid angles should show large count fluctuations, the profile averaged

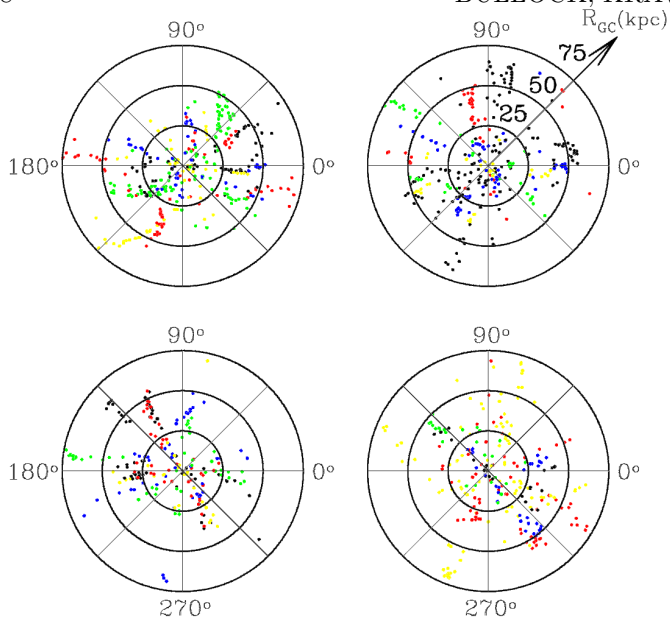


FIG. 6.— Same as Figure 5, but for a different merger history realization of the host halo. The host in this realization accreted about 20 luminous satellites over its history.

over the full sky should not cut off sharply.

Figures 5 and 6 present a different view of the structure associated with disrupted satellites, in a form more comparable to the plots of Yanny et al. (2000). Each figure shows a one degree wide, randomly oriented, great circle slice through a realization of the RR Lyrae distribution. The two figures show stellar halos for different Monte Carlo accretion histories, one with a total of about 60 tidally destroyed galaxies (Figure 5) and one with a more quiescent accretion history and about 20 tidally destroyed galaxies (Figure 6). This range roughly covers the scatter in the number of disruption events expected from galaxy to galaxy. The three concentric circles indicate galactocentric radii of 25, 50, and 75 kpc. In both figures, structures associated with the individual disrupted objects become more easily identifiable at larger radii.

To make our predictions more quantitative, we present two simple statistical measures of the halo clumpiness. Figure 7 shows the probability distribution of model RR Lyrae counts in solid angle cells of different sizes and for different ranges of galactocentric radii. The cells are roughly square on the sky; they are defined by dividing the sky map for each realization into patches of a given size. In order to take out the uncertainty in the overall amplitude of the density distribution, and to factor out the variation in the overall amplitude from one halo realization to another, the counts are presented in units of the average expected number, $\langle N \rangle$, of RR Lyrae in patches of the chosen size for each realization. Figure 7 shows that the amplitude of patch-to-patch count fluctuations is higher for smaller solid angles and for larger galactocentric

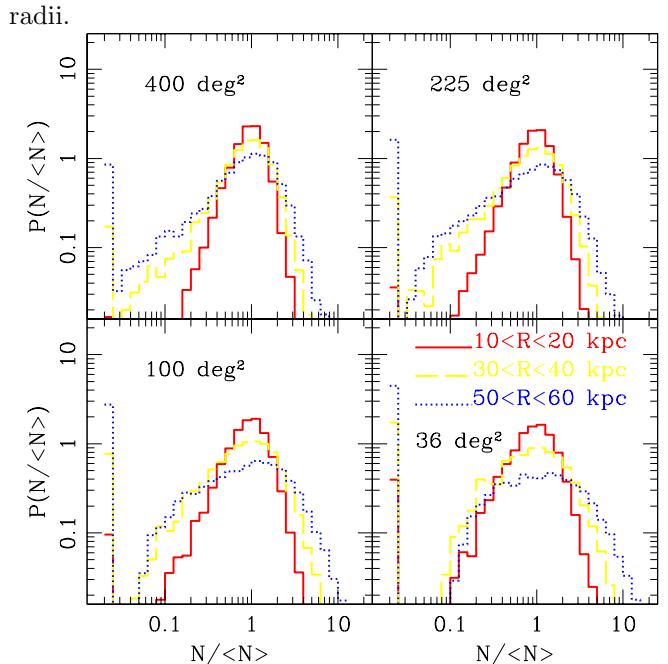


FIG. 7.— Probability distribution of simulated RR Lyrae counts in solid angle cells for various radial ranges. Here, $N/\langle N \rangle$ is the measured number of stars within the given radial bin and solid angle cell divided by the average number for a cell of that size. The cells are roughly square in angle size and were defined by dividing the sky of each realization into patches of the indicated size, with the observer at the center of the halo. The spikes at small $N/\langle N \rangle$ represent empty cells. Note that higher amplitude fluctuations from patch to patch are more likely for smaller patch areas and for larger galactocentric radii.

Figure 8 shows the rms dispersion in RR Lyrae counts, $\sigma(N/\langle N \rangle)$, as a function of galactocentric radius for cells of different solid angle and geometry. The solid points/line show counts in square cells, while open points represent the counts in one degree wide strips. The error bars for the solid points show the standard deviation of the dispersion for different merger history realizations; the error bars are similar for the open points. These error bars reinforce the point made in our illustrative figures above, namely that the degree of surviving substructure is quite variable from one realization of the stellar halo to another. The dashed lines show the expected amplitude of Poisson fluctuations based on the average number of stars expected within the given solid angle and radial bin. Note that the predicted fluctuations are always larger than Poisson fluctuations, especially at large radii, because they are dominated by fluctuations in the number of debris streams rather than \sqrt{N} fluctuations in the number of RR Lyrae. Again, the fluctuations are larger for cells of smaller solid angle and for larger radii. They are also larger for square patches than for narrow strips of the same solid angle, reflecting the fact that a narrow strip is less likely to enclose an entire disrupted object and instead encloses fragments of multiple debris streams.

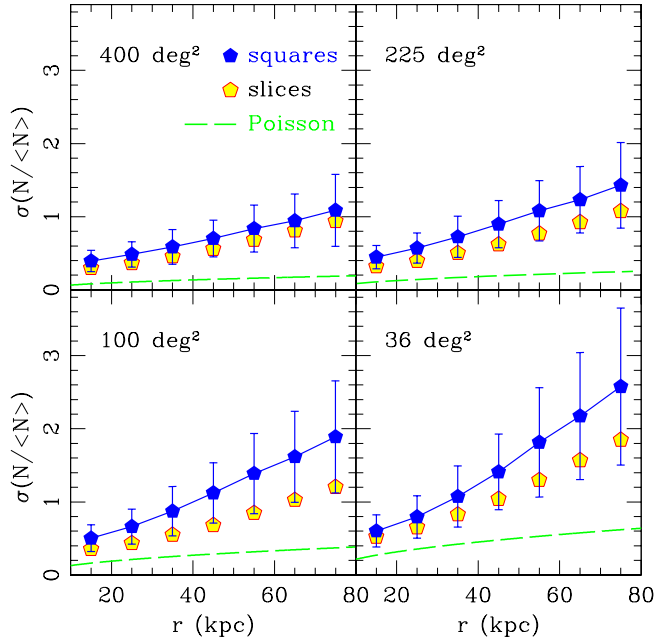


FIG. 8.— Fractional rms fluctuation of stellar counts as a function of radius for sky patches of different solid angle. The solid points are for a roughly square angular patch geometry, and the open points correspond to one degree wide strips. The error bars represent the dispersion in the rms fluctuation from realization to realization for an ensemble of merger histories. The dashed lines show the expected Poisson uncertainty based on the average number of RR Lyrae expected within the given solid angle and radial bin.

4. DISCUSSION AND CONCLUSIONS

We have presented a model in which stellar halos of Milky Way type galaxies are built via the accretion and tidal disruption of satellite galaxies. The model is based on the CDM structure formation scenario, with the crucial assumption that only a fraction of dark matter halos with circular velocities $\lesssim 30 \text{ km s}^{-1}$ are luminous and host a sizable stellar system⁴. These luminous halos are those that collapsed and accreted a substantial fraction of their mass prior to the epoch of reionization, z_{re} . Only the accretion and tidal disruption of *luminous* dwarf galaxies contribute to the build up of the stellar halo in our model.

The model predicts an average density profile for the stellar halo of $n_* \propto r^{-\alpha}$, with $\alpha \sim 3$ in the range $r \simeq 10 - 50$ kpc, in good agreement with observations. The density profiles of individual realizations of the host halo merger histories, however, exhibit a substantial scatter around this average, with the power law varying from $\alpha \sim 2.5 - 3.5$. The reason why the stellar halo density profile is steeper than that of the dark matter ($\alpha_{\text{DM}} \sim 2$, which is indeed typical of that of the *surviving* subhalos in our model), is that central satellites are more likely to be destroyed than those at large radii, since satellites far from the galactic center must have extremely eccentric orbits in order to pass close enough to be tidally destroyed. The av-

erage predicted profile falls off more steeply at $r \gtrsim 50$ kpc, but it does not have a sharp outer boundary.

The amplitude of the mean profile depends on several uncertain factors, such as the mean stellar luminosity to dark mass ratio of the disrupted dwarfs and the mean number of RR Lyrae per solar luminosity. There are also significant (factor of two) statistical fluctuations in the amplitude from one realization to another. The amplitude of the predicted RR Lyrae profile is therefore uncertain by a factor of a few. Nonetheless, with “best guess” parameter values chosen on the basis of other considerations, the mean RR Lyrae profile agrees very well with that determined by Wetterer & McGraw (1996), in slope and amplitude. It therefore appears that disruption of dwarf satellites is a plausible mechanism for producing the entire stellar halo within the CDM framework, though it could also co-exist with some other mechanism. The uncertainty in our predicted normalization is reduced by the fact that we require the model to self-consistently reproduce the velocity function of observed dwarf satellites, a point that we will return to shortly.

The main qualitative prediction of the model is the presence of significant clumpiness in the outer regions ($\gtrsim 30$ kpc) of the Galaxy’s stellar halo. This clumpiness is due to the surviving tidal debris of dozens of satellite galaxies disrupted during evolution of their host. In the inner regions of the stellar halo ($r \lesssim 30$ kpc), the density distribution is relatively smooth. At larger radii, however, the clumpiness of the stellar halo manifests itself when viewed through fixed solid angle patches in the sky. For typical modeled stellar halos, RR Lyrae profiles of the type observed by Ivezić et al. (2000) in the SDSS commissioning data (with a coherent structure at $r \sim 50$ kpc) are not uncommon.

We have quantified our predictions by presenting some statistical measures of the “clumpiness” in our modeled stellar halos. First, we measured the probability distribution (see Fig. 7) of RR Lyrae counts, $N/\langle N \rangle$, in solid angle cells of different sizes and for different galactocentric radial bins (here $\langle N \rangle$ is the average number of stars expected in a cell). We also presented the rms width of this probability distribution as a function of galactocentric radius for solid angle cells of different geometries (Fig. 8). These statistics show that the variance in the stellar counts (i.e., clumpiness of the stellar halo) increases with increasing galactocentric radius and decreasing solid angle. Although current observational data sets are not sufficiently large to derive similar statistics for comparison, future samples of RR Lyrae and A-stars from the SDSS and 2dF surveys should make such comparisons possible. For cell sizes of 36 deg^2 or larger, predicted fluctuations in RR Lyrae counts are much larger than Poisson fluctuations, at all galactocentric radii considered.

These quantitative predictions depend on some of the model assumptions. For instance, one of the implicit assumptions in our analysis is that the dark matter distribution in the host halo is nearly spherically symmetric. In particular, we do not include the possible precession of satellite orbits. In the case of the significantly oblate halo, such precession can erase signatures of the tidal tails (at least in configuration space), so it would reduce the

⁴All DM halos with circular velocities $> 30 \text{ km s}^{-1}$ are assumed to host a luminous galaxy.

predicted clumpiness of the outer halo (e.g., Ibata et al. 2000a). However, the observed narrowness of the tidal tail of the Sagittarius dwarf galaxy implies a nearly spherical halo potential at $r \lesssim 60$ kpc (Ibata et al. 2000a). A nearly spherical mass distribution in the inner region of a *galaxy-mass* halo is consistent with predictions of CDM models (Bullock et al. 2000b). We have also neglected the effects of the disk component on the background potential. Including this non-spherical central component would induce precession in the tidal orbits (Helmi & White 1999) and smear out residual structure at small galactic radii. But since this effect would only be important in the central regions ($r \lesssim 20$ kpc), the net effect would be to strengthen the trend of increased variance in star counts with radius.

The assumption that affects our predictions the most, however, is that only a small fraction of disrupted subhalos host a stellar system and thereby contribute to the build up of the stellar halo. In other words, the predicted properties of the stellar halo depend crucially on the way that we have solved the dwarf satellite problem. This problem, namely that the predicted number of dark halos with circular velocities $\lesssim 30$ km s⁻¹ is much larger than the observed number of dwarf satellites within the virialized dark halos of the Milky Way and M31 (Kauffmann et al. 1993; Klypin et al. 1999a; Moore et al. 1999), is one of the few outstanding problems of the conventional inflationary CDM model, which, with the inclusion of a cosmological constant, accounts well for a wide variety of other observational data.

Other proposed solutions to the dwarf satellite problem include modifying the inflationary fluctuation spectrum (Kamionkowski & Liddle 2000) or modifying the properties of dark matter by making it warm (WDM; e.g., Hogan & Dalcanton 2000) or self-interacting (SIDM; e.g., Spergel & Steinhardt 2000). In the SIDM model, halos collapse and accrete mass in a similar manner to conventional CDM halos. However, the number of surviving subhalos within a Milky Way mass halo is reduced because lower concentration of the SIDM halos makes them easier to disrupt and because interactions lead to “ram pressure” stripping of the dark halos. Relative to our reionization solution, the SIDM solution seems to predict a more massive and more extended stellar halo built from a larger number of tidal streams, since the abundance of dwarf satellites is reduced by a higher efficiency of satellite disruption rather than suppression of star formation in low-mass systems. Indeed, the SIDM model seems at some risk of overproducing the stellar halo. However, if the predicted stellar halo were normalized to the mean stellar density of the observed one, the SIDM model would probably predict less substructure than the model presented here because of the higher density of independent tidal streams.

The predictions of WDM and broken scale-invariance models are less clear, since they can reduce dwarf satellite numbers both by suppressing their formation in the first place (White & Croft 2000) and by making them less concentrated and therefore easier to disrupt (Colín et al. 2000). If the second effect dominates, the predictions might be closer to those of SIDM; if the first effect dominates, they might be closer to those of the reionization model. At present, we lack quantitative predictions on this matter from SIDM and WDM, and we lack detailed observational constraints, so we cannot draw conclusions

about which model fares best. However, it appears that studies of the mass, radial profile, and substructure of the stellar halo might provide useful constraints on these models in the near future.

It is interesting that all of the substructures detected in the nearly all-sky Carbon star survey and the SDSS commissioning data could be produced by a single tidal stream of the Sagittarius dwarf galaxy (Ibata et al. 2000b). In particular, the observed excess in the RR Lyrae number density profile at $r \approx 45$ kpc is caused by a clump of stars near the apocenter of the Sagittarius orbit. If most of the RR Lyrae in the surveyed strip belong to the Sagittarius stream, then no stars are expected beyond the apocenter of the Sagittarius orbit, and this would naturally explain the drop in the RR Lyrae number density at $r \gtrsim 60$ kpc detected in the SDSS data. However, the presence of only a single stream in a large volume of sky would be both puzzling and intriguing, since the CDM models considered in this paper predict at least ~ 20 (and typically more) tidal streams in the halo of a Milky Way-size galaxy. The SIDM and WDM stellar halos should be built from even larger number of tidal streams. Carbon stars are relatively young and rare, and therefore older tidal streams may not be revealed by their distribution. We predict, however, that many more substructures not associated with the Sagittarius tidal stream should be detected in the future as the SDSS covers a larger area of the sky. Absence of such detections would spell serious trouble for CDM models, and possibly even more so for the variants of CDM that we have discussed.

Several past theoretical studies of tidal stripping and disruption of galactic satellites have shown that tidal streams can be used as powerful probes of both the present potential of the Milky Way (Johnston et al. 1999; Ibata et al. 2000a) and its accretion history (e.g., Helmi & White 1999; Helmi et al. 1999; Helmi & de Zeeuw 2000). For example, Johnston et al. (1999) show that parameters characterizing the mass distribution in the Milky Way halo can be determined with an accuracy of a few percent using a single tidal stream if accurate phase-space information is available for as few as 100 stream stars. Helmi et al. (1999) show how phase-space information can be used to recover fossil remnants of the satellites accreted and disrupted early in the Milky Way evolution. These techniques can be used to construct a detailed formation history of the Galaxy.

In this study, we have focused on the spatial distribution of stars in the Milky Way halo. The radial density behavior of stars may not prove to be as sensitive a probe of the galactic potential as the accurate phase-space mapping of tidal streams (Johnston et al. 1999), but it should be very useful in recovering details of the Milky Way accretion history. In some respects, the number of surviving tidal streams or the degree of clumpiness of the stellar distribution can provide better constraints on the variants of the CDM scenario than the abundance of galactic satellites. An advantage here is that the spatial distribution of halo stars should be possible to map in the very near future, when large samples of halo stars from the SDSS and other surveys become available. Accurate, large-scale, phase-space mapping of tidal streams, on the other hand, will become possible only after launch of the next generation astrometric space missions (i.e., at the end of the decade).

On the theoretical side, our model and predictions can be improved upon by combining mass accretion histories typical for the galaxy-size halos formed in CDM models with more sophisticated numerical models of orbital evolution of satellites and their tidal debris.

We thank Amina Helmi and Kathryn Johnston for useful discussion and suggestions. This work was supported in part by NASA LTSA grant NAG5-3525 and NSF grant AST-9802568. Support for A.V.K. was provided by NASA through Hubble Fellowship grant HF-01121.01-99A from the Space Telescope Science Institute, which is operated by the Association of Universities for Research in Astronomy, Inc., under NASA contract NAS5-26555.

REFERENCES

- Arnold, R., & Gilmore, G., 1992, MNRAS, 257, 225
 Barkana, R., & Loeb, A. 1999, ApJ, 523, 54
 Binney, J., & Merrifield, M., 1998, Galactic Astronomy (Princeton: Princeton University Press)
 Bond, J. R., Cole, S., Efstathiou, G., Kaiser, N., 1991, ApJ, 379, 440
 Brocato, E., Buonanno, R., Malakhova, Y., & Piersimoni, A. M., 1996, A&A, 311, 778
 Bullock, J.S., Flores, R., Kolatt, T.S., Kravtsov, A.V., Klypin, A., & Primack, J.R.. 2000b, in preparation.
 Bullock, J.S., Kolatt, T.S., Sigad, Y., Somerville, R.S., Kravtsov, A.V., Klypin, A., Primack, J.R., & Dekel, A. 2000a, MNRAS, submitted (astro-ph/9908159)
 Bullock, J.S., Kravtsov, A.V., & Weinberg, D.H., ApJ, accepted, astro-ph/0002214, BKW
 Burles, S., & Tytler, D. 1998, ApJ, 507, 732
 Colín, P. Avila-Reese, V., Valenzuela, O. 2000, ApJ submitted (astro-ph/0004115)
 Colpi, M., Mayer, L., & Governato, F. 1999, ApJ, 525, 720.
 Davé, R., Spergel, D.N., Steinhardt, P.J., Wandelt, B.D. 2000, ApJ submitted (astro-ph/0006218)
 Eggen, O.J., Lynden-Bell, D., & Sandage, A.R., 1962, ApJ, 136, 748
 Evans, C. R., & Kochanek, C. S., 1989, ApJ, 346, L13
 Ghigna, S., Moore, B., Governato, F., Lake, G., Quinn, T., & Stadel, J. 1998, MNRAS, 300, 146
 Gould, A., Guhathakurta, P., Richstone, D., & Flynn, C., 1992, ApJ, 388, 345
 Hawkins, M.R.S. 1984, MNRAS 206, 433
 Helmi, A., & White, S.D.M. 1999, MNRAS 307, 495
 Helmi, A., White, S.D.M., de Zeeuw, P.T., & Zhao, H.-S. 1999, Nature, 402, 53
 Helmi, A., & de Zeeuw, P.T. 2000, MNRAS submitted, astro-ph/0007166
 Hogan, C.J., & Dalcanton, J.J. 2000, Phys.Rev. D, in press (astro-ph/0002330)
 Ibata, R., Lewis, G.F., Irwin, M., Totten, E., Quinn, T. 2000a, astro-ph/0004011
 Ibata, R., Irwin, M., Lewis, G.F., Stolte, A. 2000b, ApJL submitted (astro-ph/0004255)
 Ibata, R.A., & Razoumov A.O. 1998, A&A, 336, 130
 Irwin, M., & Hatzidimitriou, D., 1995, MNRAS, 277, 1354
 Ivezić, Ž, et al., 2000, AJ, submitted, astro-ph/0004130
 Johnston, K.V., 1998, ApJ, 495, 297
 Johnston, K.V., Spergel, D.N. & Hernquist, L. 1995, ApJ, 451, 598
 Johnston, K.V., Zhao, H., Spergel, D.N., Hernquist, L. 1999, ApJ, 512, L109
 Kamionkowski, M., & Liddle, A.R. 1999, preprint (astro-ph/9911103)
 Kauffmann, G., White, S.D.M., & Guiderdoni, B. 1993, MNRAS, 264, 201
 Klypin, A.A., Kravtsov, A.V., Valenzuela, O., & Prada, F. 1999a, ApJ, 522, 82
 Klypin, A.A., Gottlber, S., Kravtsov, A.V., & Khokhlov, A.M. 1999b, ApJ, 516, 530
 Kuhn, J. R., Smith, H. A., & Hawley, S. L., 1996, ApJ, 469, L93
 Lacey, C., & Cole, S., 1993, MNRAS, 262, 627 (LC93)
 Layden, A.C., 1998, in ASP Conf. Ser. 136, Galactic Halos, ed. D. Zaritsky, (San Fransico:ASP), 14
 Majewski, S.R., Munn, J.A., & Hawley, S.L, 1994, ApJ, 427, L37
 Majewski, S.R., Munn, J.A., & Hawley, S.L, 1996, ApJ, 459, L73
 Majewski, S.R., Ostheimer, J.C., Patterson, R.J., Kunkel, W.E., Johnston, K.V., Geisler, D. 2000, AJ 119, 760
 Mateo, M.L. 1998, ARA&A, 36, 435
 Moore, B., Ghigna, F., Governato, F., Lake, G., Stadel, J., & Tozzi, P. 1999, ApJ, 524, L19
 Narayanan, V.K., Spergel, D.N., Davé, R., Ma, C.-P. 2000, ApJ, submitted (astro-ph/0005095)
 Navarro, J.F., Frenk, C.S., White, S.D.M. 1997, ApJ, 490, 493
 Press, W.H., & Schechter, P. 1974, ApJ, 187, 425
 Preston, G.W., Schectman, S.A., & Beers, T.C., 1991, ApJ, 375, 121.
 Preston, G.W., Beers, T.C., & Schectman, S.A., 1994, AJ, 108, 538
 Searle, L., 1977, in The Evolution of Galaxies and Stellar Populations, ed. B.M. Tinsley & R.B. Larson (New Haven: Yale University Press), 219
 Searle, L. & Zinn, R., 1978, APJ, 225, 357
 Somerville, R.S., & Kolatt, T.S. 1999, MNRAS, 305, 1 (SK99)
 Spergel, D.N., & Steinhardt, P.J. 1999, preprint (astro-ph/9909386)
 Wetterer, C.J., & McGraw, J.T. 1996, AJ, 112, 1046
 White, M., & Croft, R.A., 2000, ApJ, submitted, astro-ph/0001247
 Wyse, R. F. G. 1999a, in ASP Conf. Ser. 165: The Third Stromlo Symposium: The Galactic Halo, 1
 Wyse, R. F. G. 1999b, in The formation of galactic bulges, ed. C.M. Carollo, H.C. Ferguson, R.F.G. Wyse, (Cambridge: Cambridge)
 Yanny, B., et al., 2000, ApJ, accepted, astro-ph/0004128
 York, D.G., et al., 2000, AJ, accepted, astro-ph/0006396